

Enhanced emission efficiency in electrospun polyfluorene copolymer fibers

Giovanni Morello,^{1,2,a)} Alessandro Polini,^{1,b)} Salvatore Girardo,¹ Andrea Camposeo,^{1,2,a)} and Dario Pisignano^{1,2,3}

¹National Nanotechnology Laboratory of Istituto Nanoscienze-CNR, via Arnesano, I-73100 Lecce, Italy

²Center for Biomolecular Nanotechnologies @UNILE, Istituto Italiano di Tecnologia, Via Barsanti, I-73010 Arnesano (LE), Italy

³Dipartimento di Matematica e Fisica "Ennio De Giorgi," Università del Salento, via Arnesano, I-73100 Lecce, Italy

(Received 29 January 2013; accepted 14 May 2013; published online 30 May 2013)

We report on the unique emission features of light-emitting fibers made of a prototype conjugated polymer, namely, poly[(9,9-dioctylfluorenyl-2,7-diyl)-*co*-(1,4-benzo-{2,1'-3}-thiadiazole)] (F8BT), realized by electrospinning with diameters in the range of 500-1000 nm. The fibers display emission polarized along their axis, evidencing a favoured alignment of the polymer molecules. Emission efficiency and time resolved measurements reveal an enhancement of both the quantum efficiency and the radiative rate (up to 22.5%) of the fibers compared to spin-coated films, shedding more light on their potential as miniaturized photon sources in optoelectronic devices requiring high recombination rates. © 2013 AIP Publishing LLC. [<http://dx.doi.org/10.1063/1.4807894>]

Conjugated polymers have received a growing interest due to their high potential for application in many technological fields. They are intriguing materials on both the fundamental and application point of view. Till now, several applications have been implemented exploiting conjugated polymers as active media, including organic light-emitting diodes (OLEDs),¹ photovoltaic cells,² and field-effect transistors.³ The photophysics of these materials has been investigated a lot in the last decade⁴⁻⁸ in an attempt to rationalize the phenomena associated with charge and energy migration, especially in solid state samples, and to finally improve the performances of the developed devices. A distinctive feature of this class of polymers is the dependence of their optoelectronic properties on the peculiar micro/nanoscale structure and morphology.^{9,10} For these reasons, most of the recent research has been dedicated to micro and nanostructured conjugated polymers, in which molecular backbones can be oriented and/or stretched along a preferential axis.¹¹⁻¹⁵ This orientation may induce changes in important physical properties and in their associated mechanisms, such as the charge transport,^{16,17} photoluminescence (PL) anisotropy,^{15,18-21} and energy transfer.^{4,22} Among the micro and nanostructures made of conjugated polymers, electrospun fibers are rapidly emerging as quasi 1-dimensional (1-D) class of active nanomaterials. In these systems, the electric-field-induced stretching and the elongation of the polymer solution during the electrospinning process²³ are likely to favour a preferential alignment of the polymer backbones along the fiber longitudinal axis. Polarized Raman, infrared, and photoluminescence spectroscopies have evidenced such molecular alignment,^{13,16,18,24} and ordered arrays of electrospun nanofibers made by conjugated polymers have been

proposed as effective polarized light sources.²⁵ Importantly, the molecular packing in the stretched fiber structure can also affect the radiative rate, which is in turn sensitive to the dielectric tensor of the environment around the emitting chromophores,²⁶ to the coupling to vibrational modes,²⁷ to the molecular conformational properties,^{28,29} and to variations of the conjugation length.³⁰ However, the intrinsic radiative rates of chromophores within fibers fully made of conjugated polymers are still unexplored, whereas a lot of studies have been limited to the analysis of the emission peak wavelengths and spectral lineshape.^{18,31-33} In this work, we report on the radiative rate in electrospun fibers made of a prototype conjugated polymer, largely used as active medium of organic devices,^{34,51} namely, the poly[(9,9-dioctylfluorenyl-2,7-diyl)-*co*-(1,4-benzo-{2,1'-3}-thiadiazole)] (F8BT, chemical structure reported in Fig. 1(a)) from which beadless, highly luminescent fibers with diameters ranging from 500 nm to 1 μ m are produced (Figs. 1(b) and 1(c)). By measuring the PL quantum yield (PLQY) and the PL decay time, we find a clear evidence for an increase of the radiative rate (up to 22.5%) in the fiber structures made by conjugated polymer solutions under strong elongation flows, compared to microscopically unordered films made by spin-coating. These findings suggest a strategic route to increase emission quantum yield and polarization performances of conjugated polymers in solid state emitting systems, with a possible important impact in designing future light-emitting devices based on organic semiconducting materials.

The fabrication of conjugated polymer nanofibers by electrospinning has been reported elsewhere.^{18,35} Here, the polymer solution is prepared with a concentration of 1.4×10^{-3} M by using tetrahydrofuran (THF) as solvent. The use of a single-solvent system (dielectric constant, $\epsilon = 7.5$, boiling point, $T_{bp} = 66^\circ\text{C}$) allows the formation of a homogeneous spinning solution, able to produce uniform fibers for applied voltages in the range 5–15 kV. The morphology of fibrous samples is imaged by scanning electron microscopy (SEM) with a Nova

^{a)}Authors to whom correspondence should be addressed. Electronic addresses: giovanni.morello@nano.cnr.it and andrea.camposeo@nano.cnr.it.

^{b)}Present address: Materials Sciences Division, Lawrence Berkeley National Laboratory, 1 Cyclotron Road, MS 62-0203, Berkeley, California 94720, USA.

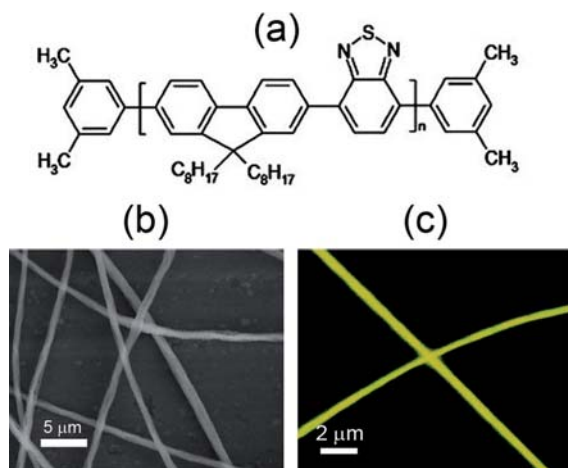


FIG. 1. (a) Chemical structure of F8BT (from American Dye Source datasheet). (b) SEM image, representative of the sample. (c) Confocal microscopy image of two single electrospun fibers.

NanoSEM 450 system (FEI) using an acceleration voltage of 10 kV without prior metallization (Fig. 1(b)). Confocal microscopy characterization is performed by placing the fibers on a glass coverslip and exciting them by a diode laser operating at 405 nm (Fig. 1(c)). In order to reduce diffraction-induced limitations, the measurements are performed by means of a high numerical aperture objective lens (oil immersed, 60 \times , NA = 1.4) employed as exciting and collecting means. PLQY and absorption measurements are performed by the use of an integrating sphere.³⁶ The excitation consists in a diode laser (405 nm) for PLQY measurements. For evaluating the absorption spectrum, we use a W lamp. In both cases the signal is detected by an air-cooled CCD. *Polarized* micro-PL characterization is carried out by means of an optical microscope equipped with an UV mercury lamp ($\lambda < 450$ nm) coupled to an objective lens (50 \times , NA = 0.75) for the photoexcitation. Light emitted by the fibers, passing through a rotating polarization analyser placed across the optical path, is detected by a CCD camera (450 Leica, DFC 490). Time resolved PL measurements are performed in single-photon counting mode by

exciting the samples at a low excitation level by a light-emitting diode (LED) source ($\lambda = 338$ nm) with a repetition rate of 1 kHz. The instrumental response function (IRF) is taken into account by a calibrated deconvolution procedure.

In order to investigate the potential alignment of polymer chains within the electrospun fibers, we perform *polarized* micro-PL measurements, finding evidence of a quite higher degree of polarization of emission from fibers compared to disordered (film) system. In Fig. 2(a), we report the PL intensity vs. analyser angle of F8BT single fiber, and the corresponding best fit to the Malus' expression

$$I(\theta) = I_{\min} + I_0 \cos^2(\theta), \quad (1)$$

where I_{\min} stands for the minimum measured intensity and $(I_0 + I_{\min})$ corresponds to the maximum intensity. The polarization factor, r , is calculated as

$$r = \frac{I_{\max} - I_{\min}}{I_{\max} + I_{\min}} = \frac{I_0}{I_0 + 2I_{\min}}. \quad (2)$$

Compared to spin-coated film, for which a relative small polarization factor is measured ($\sim 14\%$, likely related to statistical fluctuation), F8BT fibers display a polarization factor up to 51%. Since the polarization factor is strictly related to the alignment of the transition dipole moments of the emitting species, these findings highlight an enhanced ordering of the emitting chromophores along the fiber longitudinal axis.

Fig. 3(a) compares the absorption and PL spectra of film and fibers. The PL is collected at room temperature and under low excitation density (~ 100 mW/cm²) to prevent photodegradation³⁷ and bimolecular effects.³⁸ The absorption spectrum of the fibers is comparable to that of the reference film, with almost identical positions of the main peaks, revealing a common origin of the optical transitions in both the systems. The main difference is a broadening of the fibers absorption spectrum at low energies. Noticeably, the PL of F8BT fibers is blueshifted compared to that of films, by about 10 nm. The contribution of self-absorption to the observed PL blueshift can be ruled out, as discussed in the following. Fig. 3(b) displays the PL decay curve of the fibrous sample. The fibers PL decay follows an exponential trend (similar results are obtained for the PL decay of the film), without evidence for bimolecular processes which would accelerate the decays leading to an incorrect estimate of the decay rates.

The analysis of the PL temporal decay data evidences a longer luminescence lifetime for fibers compared to film. In particular, the extracted values are (1.3 ± 0.1) ns for the film and (1.5 ± 0.1) ns for the fibers (Table I). These results suggest that the packing of the conjugated polymer molecules and hence the structural organization of emitting chromophores in the fibrous system has an impact also on the excited states lifetime. In order to better investigate this issue, we evaluate the radiative rate of the investigated samples through the measurement of the PLQY (hereafter referred to as Φ) and of the PL lifetime (τ_{obs}), which allows to calculate the intrinsic radiative and nonradiative decay times as follows:

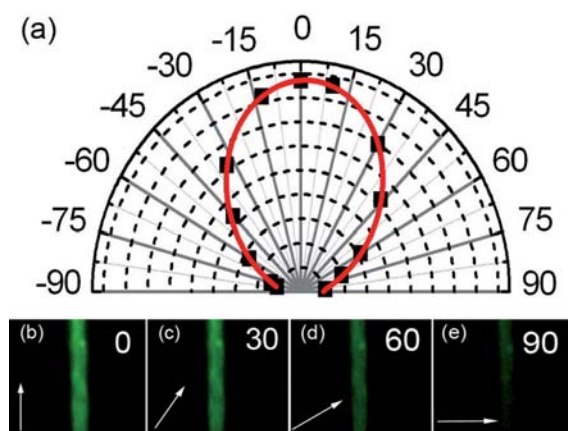


FIG. 2. (a) Polarized PL intensity vs. the analyzer angle (measured with respect the fiber axis) of a single F8BT fiber (symbols) and relative best fit to Eq. (1). The emission intensity is maximum when the analyzer axis is parallel to the fiber length ($\theta = 0^\circ$). (b)–(e) Fluorescence micrographs of the fiber at the different polarization angles. The white arrow indicates the analyzer position with respect to the fiber axis.

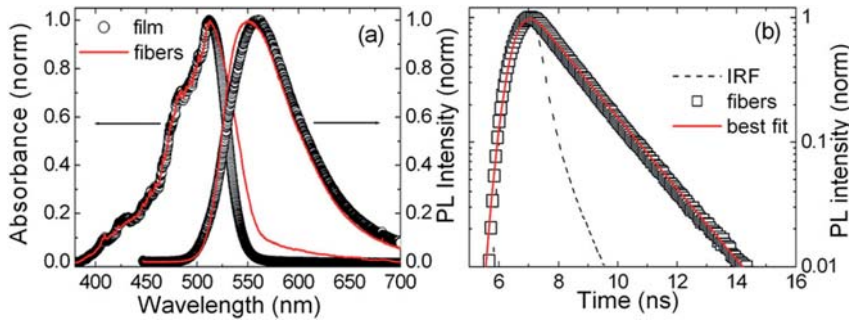


FIG. 3. (a) Comparison between the normalized absorbance (left vertical scale) and PL (right scale) spectra of F8BT fibers (red lines) and film (black symbols). (b) PL temporal trace of F8BT fibers (symbols) and corresponding best fit (red continuous line) to an exponential function convoluted with the Instrumental Response Function (dashed line) on a semi-log scale.

$$\Phi = \frac{\tau_{obs}}{\tau_{rad}}, \quad \frac{1}{\tau_{obs}} = \frac{1}{\tau_{rad}} + \frac{1}{\tau_{nrad}} \iff \tau_{rad} = \frac{\tau_{obs}}{\Phi}, \quad (3)$$

where τ_{obs} is the measured PL lifetime, τ_{rad} and τ_{nrad} are the intrinsic radiative and nonradiative lifetimes, respectively. The measured values of Φ are (0.27 ± 0.01) for the film and (0.40 ± 0.01) for the fibers, from which we deduce the values of radiative and non radiative lifetime by applying Eq. (3). The spin-coated film is characterized by $\tau_{rad} = (4.9 \pm 0.1)$ ns and $\tau_{nrad} = (1.8 \pm 0.1)$ ns, whereas the fibers present $\tau_{rad} = (3.8 \pm 0.1)$ ns and $\tau_{nrad} = (2.5 \pm 0.1)$ ns. Both Φ and the time constants well agree with literature data ($\Phi \sim 0.4$, $\tau > 1$ ns),^{39,40} whereas the observed PL lifetimes are comparable to those of similar systems, in which the principal nonradiative decay channel is the formation of triplet states.⁴¹ Interestingly, the polymer fibers display a significant *increase of the radiative rate* with respect to films (0.26 ns^{-1} against 0.2 ns^{-1}). In conjugated polymers the ideal infinite conjugation of π -orbital delocalized in one dimension is interrupted by a series of twists and kinks so that the polymer chain results in an ensemble of conformational sub-units which are considered the base chromophores for the light emission. They are constituted, in turn, by a number of single repeated units (up to 10) and thus feature different conjugation lengths. Their distribution is the main cause of the inhomogeneous broadening (observable in absorption and partially in PL) and their mutual interaction contributes to the formation of delocalized collective states. Recent works have evidenced that the absorption of light in conjugated polymers promotes the system in excited delocalized states^{8,42} and in a time scale of 100–200 fs (Ref. 8) the excitation localizes in a sub-unit, not necessarily the longest one (at lowest energy). For longer timescale (from a few to hundreds of picoseconds) hopping mechanisms due to electronic energy transfer (EET) occur, leading the excitons towards sites at lower energy until reaching the longest sub-unit.^{8,43,44} The final populated state can in turn decay radiatively or non-radiatively into other further redshifted traps, aggregates, and/or triplet states. In particular, aggregation effects can occur

depending on the processing physics (employed solvent, phase separation, induced aggregation), favoring the formation of interchain states that exhibit a low quantum yield and a redshifted, long-living emission.^{9,45}

The enhanced alignment of the polymer chains in fibers (Fig. 4) can contribute to weaken the interaction among neighbouring chromophores responsible for interchain excited states formation and to reduce exciton migration towards low-energy sites. Such decreased exciton migration induces a blueshifted PL in fibers as shown in Fig. 3(a) and reported in other works for a number of different polymers^{31,32,46} and a consequent increase of the efficiency and the nonradiative lifetime. As a further possible cause contributing to the shape of the PL spectrum, the self-absorption process (typical of materials having a nonzero absorption/PL overlap) has to be taken into account. In fact, this mechanism would result in the fictitious redshift of the emission in systems where the process is more efficient, together with a reduction of the measured efficiency and lengthening of lifetime. Different polymers (and morphologies)⁴⁷ show a different attitude to re-absorption, generally increasing with the sample thickness.^{46,48} In order to rule out a significant re-absorption, we perform PL measurements on spin-coated films with thickness of 1–4 μm finding a spectral shift lower than 1 nm, consistent with previous characterization work,⁴⁶ reporting small spectral variations in F8BT upon varying the sample thickness. The enhancement of both the PL efficiency and the measured lifetime observed for the F8BT fibers can be also attributed to the net alignment of the polymer backbones along the fiber axis, which can lead to an either less or more pronounced planarization of the benzothiadiazole (BT) and polyfluorene (F8) sub-units in the fiber compared to the film. In fact, studies on F8BT on pristine and annealed film^{51,52} have evidenced that the processing conditions of the polymer film, such as an annealing treatment after the spin-coating, strongly influence the resulting molecular packing and optoelectronic properties. For instance, in annealed films

TABLE I. List of the physical quantities measured (efficiency, Φ , and τ_{obs}) and extracted by the analysis (τ_{rad} and τ_{nrad}).

	Film	Fibers
Φ	0.27 ± 0.01	0.40 ± 0.01
τ_{obs} (ns)	1.3 ± 0.1	1.5 ± 0.1
τ_{rad} (ns)	4.9 ± 0.1	3.8 ± 0.1
τ_{nrad} (ns)	1.8 ± 0.1	2.5 ± 0.1

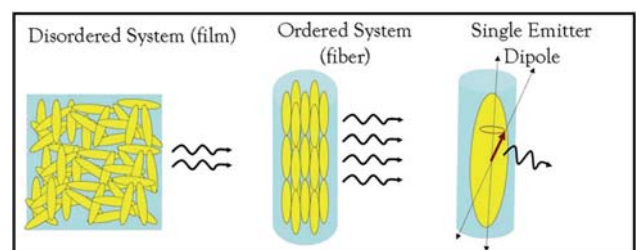


FIG. 4. Schematic representation of the polymer molecular arrangement in amorphous bulk and partially aligned, fiber microstructures.

a more planar and energetically favourable configuration is envisioned compared to pristine films, characterized by a reduced torsional angle between the F8 and BT sub-units and by a reorganization of the sub-units in a so-called “alternating structure.”⁵¹ Such more planar molecular packing is found to produce a slight broadening of the absorption spectrum towards longer wavelengths and a blueshift of the emission with respect to pristine films, similarly to the observed optical properties of the fibers. The PL line-shape and peak energy originate from the particular interplay between the multiple emissive states population and the electronic energy transfer among them. Donley *et al.* have found a less efficient energy transfer in planar configuration, corresponding to a net blueshifted PL and an increase of the quantum efficiency.⁵¹ The present results suggest a more planar and energetically favourable configuration of the F8 and BT sub-units in the fibers with respect to spin-coated film, likely due to the peculiar dynamics of the process, involving a fast stretching of the polymer solution during the electrospinning.⁵² Such a difference in the polymer packing is also consistent with the faster PL decay observed in film, together with the enhanced PLQY of the fiber system.^{49,51,53}

In light of the extracted lifetime values, we consider that a main limitation to a very high PLQY is the formation of triplet states, by the intersystem crossing process. Such states are optically forbidden and their nature of low energy states could compete with the intrinsic decay process on what concerns the capture of the charge carriers.⁴¹ Their radiative lifetime is on the order of micro-milliseconds and also their nonradiative population, corresponding to the quenching of singlet excitons by triplet ones, is quite slow and estimated in 1-2 ns.⁴¹ Actually, this quenching lifetime is consistent to our measured nonradiative decay times, and the slight differences between the two systems studied can reflect the diverse generation efficiency of triplet states. Recent pump-probe time resolved experiments have evidenced the occurrence of less efficient intersystem crossing in F8BT in planar arrangement compared to a molecular configuration with higher torsional angles between F8 and BT sub-units, due to the reduced mixing between the σ and π orbitals.⁵³ Such findings are consistent with the longer nonradiative lifetime and higher quantum efficiency measured in F8BT fibers compared to films.

In conclusion, the elongation conditions and whipping/stretching instabilities typical of fiber-production processes as electrospinning, namely, the continuous jet-thinning and correlated faster solvent evaporation rate,⁵⁰ induce an alignment of the polymer molecules along the fiber longitudinal axis, and a F8 and BT sub-units arrangement corresponding to an increase of both the radiative rate and the quantum efficiency with respect to films. This study demonstrates the possibility to obtain an enhancement of the radiative rate in fully conjugated polymer systems relying on fiber architectures. The net reduction of the intrinsic radiative lifetime is demonstrated by moving from disordered (spin-coated films) to more ordered (fibers) organic systems. Future work will aim to assess the generality of these results or their dependence on the specific conjugated polymer system. As an implicit outcome, our results suggest that the optimization of the fiber

fabrication conditions (further reducing the fiber diameter and the presence of defect centres) provides a route to improve the optical properties of emitting solid state polymer nanostructures in terms of PL efficiency, radiative rate, and polarization factor.

We acknowledge the financial support from the Italian Minister of University and Research FIRB RBF08DJZI “Futuro in Ricerca.” The Apulia Regional Network of Public Research Laboratories No. 09 (WAFITECH) is also acknowledged for SEM measurements.

- ¹J. H. Burroughes, D. D. C. Bradley, A. R. Brown, R. N. Marks, K. Mackay, R. H. Friend, P. L. Burns, and A. B. Holmes, *Nature* **347**, 539 (1990).
- ²G. Li, R. Zhu, and Y. Yang, *Nat. Photonics* **6**, 153 (2012).
- ³H. Koezuka, A. Tsumura, and T. Ando, *Synth. Met.* **18**, 699 (1987).
- ⁴T.-Q. Nguyen, J. Wu, V. Doan, B. J. Schwartz, and S. H. Tolbert, *Science* **288**, 652 (2000).
- ⁵E. Collini and G. D. Scholes, *Science* **323**, 369 (2009).
- ⁶J. C. Bolinger, M. C. Traub, T. Adachi, and P. F. Barbara, *Science* **331**, 565 (2011).
- ⁷J. Vogelsang, T. Adachi, J. Brazard, D. A. V. Bout, and P. F. Barbara, *Nat. Mater.* **10**, 942 (2011).
- ⁸I. Hwang and G. D. Scholes, *Chem. Mater.* **23**, 610 (2011).
- ⁹T.-Q. Nguyen, I. B. Martini, J. Liu, and B. J. Schwartz, *J. Phys. Chem. B* **104**, 237 (2000).
- ¹⁰D. Beljonne, G. Pourtois, C. Silva, E. Hennebicq, L. M. Herz, R. H. Friend, G. D. Scholes, S. Setayesh, K. Müllen, and J. L. Brédas, *Proc. Natl. Acad. Sci.* **99**, 10982 (2002).
- ¹¹F. S. Kim, G. Ren, and S. A. Jenekhe, *Chem. Mater.* **23**, 682 (2011).
- ¹²D. Li, A. Babel, S. A. Jenekhe, and Y. Xia, *Adv. Mater.* **16**, 2062 (2004).
- ¹³L. M. Bellan and H. G. Craighead, *Polymer* **49**, 3125 (2008).
- ¹⁴H.-M. Liem, P. Etchegoin, K. S. Whitehead, and D. D. C. Bradley, *Adv. Funct. Mater.* **13**, 66 (2003).
- ¹⁵Z. Zheng, K.-H. Yim, M. S. M. Saifullah, M. E. Welland, R. H. Friend, J.-S. Kim, and W. T. S. Huck, *Nano Lett.* **7**, 987 (2007).
- ¹⁶D. Tu, S. Pagliara, A. Camposeo, L. Persano, R. Cingolani, and D. Pisignano, *Nanoscale* **2**, 2217 (2010).
- ¹⁷H. Sirringhaus, R. J. Wilson, R. H. Friend, M. Inbasekaran, W. Wu, E. P. Woo, M. Grell, and D. D. C. Bradley, *Appl. Phys. Lett.* **77**, 406 (2000).
- ¹⁸S. Pagliara, M. S. Vitiello, A. Camposeo, A. Polini, R. Cingolani, G. Scamarcio, and D. Pisignano, *J. Phys. Chem. C* **115**, 20399 (2011).
- ¹⁹D. O’Carroll, D. Iacopino, and G. Redmond, *Adv. Mater.* **21**, 1160 (2009).
- ²⁰D. O’Carroll and G. Redmond, *Chem. Mater.* **20**, 6501 (2008).
- ²¹C. De Marco, E. Mele, A. Camposeo, R. Stabile, R. Cingolani, and D. Pisignano, *Adv. Mater.* **20**, 4158 (2008).
- ²²M. C. Traub, G. Lakhwani, J. C. Bolinger, D. V. Bout, and P. F. Barbara, *J. Phys. Chem. B* **115**, 9941 (2011).
- ²³S. V. Fridrikh, J. H. Yu, M. P. Brenner, and G. C. Rutledge, *Phys. Rev. Lett.* **90**, 144502 (2003).
- ²⁴K. Yin, L. Zhang, C. Lai, L. Zhong, S. Smith, H. Fong, and Z. Zhu, *J. Mater. Chem.* **21**, 444 (2011).
- ²⁵S. Pagliara, A. Camposeo, A. Polini, R. Cingolani, and D. Pisignano, *Lab Chip* **9**, 2851 (2009).
- ²⁶S. Bhattacharya, B. Paramanik, and A. Patra, *J. Phys. Chem. C* **115**, 20832 (2011).
- ²⁷L. O’Neill, P. Lynch, M. McNamara, and H. J. Byrne, *Polymer* **49**, 4109 (2008).
- ²⁸T.-W. Lee, O. O. Park, J.-J. Kim, J.-M. Hong, and Y. C. Kim, *Chem. Mater.* **13**, 2217 (2001).
- ²⁹V. Sivamurugan, K. Kazlauskas, S. Jursenas, A. Gruodis, J. Simokaitiene, J. V. Grazulevicius, and S. Valiyaveetil, *J. Phys. Chem. B* **114**, 1782 (2010).
- ³⁰A. J. Tilley, S. M. Danczak, C. Browne, T. Young, T. Tan, K. P. Ghiggino, T. A. Smith, and J. White, *J. Org. Chem.* **76**, 3372 (2011).
- ³¹Z. Zhu, L. Zhang, S. Smith, H. Fong, Y. Sun, and D. Gosztola, *Synth. Met.* **159**, 1454 (2009).
- ³²R. Zhou, W. Chen, X. Jiang, S. Wang, and Q. Gong, *Appl. Phys. Lett.* **96**, 133309 (2010).
- ³³M. C. Gwinner, S. Khodabakhsh, M. H. Song, H. Schweizer, H. Glessen, and H. Sirringhaus, *Adv. Funct. Mater.* **19**, 1360 (2009).

- ³⁴J. Zaumseil, C. L. Donley, J.-S. Kim, R. H. Friend, and H. Sirringhaus, *Adv. Mater.* **18**, 2708 (2006).
- ³⁵F. Di Benedetto, A. Camposeo, S. Pagliara, E. Mele, L. Persano, R. Stabile, R. Cingolani, and D. Pisignano, *Nat. Nanotechnol.* **3**, 614 (2008).
- ³⁶J. C. de Mello, H. F. Wittmann, and R. H. Friend, *Adv. Mater.* **9**, 230 (1997).
- ³⁷M. Yan, L. J. Rothberg, F. Papadimitrakopoulos, M. E. Galvin, and T. M. Miller, *Phys. Rev. Lett.* **73**, 744 (1994).
- ³⁸D. Peckus, A. Devizis, D. Hertel, K. Meerholz, and V. Gulbinas, *Chem. Phys.* **404**, 42 (2012).
- ³⁹M. Watanabe, N. Yamasaki, T. Nakao, K. Masuyama, H. Kubo, A. Fujii, and M. Ozaki, *Synth. Met.* **159**, 935 (2009).
- ⁴⁰A. J. Cadby, R. Dean, C. Elliot, R. A. L. Jones, A. M. Fox, and D. G. Lidzey, *Adv. Mater.* **19**, 107 (2007).
- ⁴¹J. Yu, R. Lammi, A. J. Gesquiere, and P. F. Barbara, *J. Phys. Chem. B* **109**, 10025 (2005).
- ⁴²W. J. D. Beenken and T. Pullerits, *J. Phys. Chem. B* **108**, 6164 (2004).
- ⁴³D. Beljonne, E. Hennebicq, C. Daniel, L. M. Herz, C. Silva, G. D. Scholes, F. J. M. Hoeben, P. Jonkheijm, A. P. H. J. Schenning, S. C. J. Meskers, R. T. Phillips, R. H. Friend, and E. W. Meijer, *J. Phys. Chem. B* **109**, 10594 (2005).
- ⁴⁴E. Hennebicq, G. Pourtois, G. D. Scholes, L. M. Herz, D. M. Russell, C. Silva, S. Setayesh, A. C. Grimsdale, K. Müllen, J.-L. Brédas, and D. Beljonne, *J. Am. Chem. Soc.* **127**, 4744 (2005).
- ⁴⁵M. Yan, L. J. Rothberg, E. W. Kwock, and T. M. Miller, *Phys. Rev. Lett.* **75**, 1992 (1995).
- ⁴⁶S. Pagliara, A. Camposeo, R. Cingolani, and D. Pisignano, *Appl. Phys. Lett.* **95**, 263301 (2009).
- ⁴⁷Y. Ishii and H. Murata, *J. Mater. Chem.* **22**, 4695 (2012).
- ⁴⁸B. Ruhstaller, J. C. Scott, P. J. Brock, U. Scherf, and S. A. Carter, *Chem. Phys. Lett.* **317**, 238 (2000).
- ⁴⁹X.-F. Wu, Y. Salkovskiy, and Y. A. Dzenis, *Appl. Phys. Lett.* **98**, 223108 (2011).
- ⁵⁰D. Kabra, L. P. Lu, M. H. Song, H. J. Snaith, and R. H. Friend, *Adv. Mater.* **22**, 3194 (2010).
- ⁵¹C. L. Donley, J. Zaumseil, J. W. Andreasen, M. M. Nielsen, H. Sirringhaus, R. H. Friend, and J.-S. Kim, *J. Am. Chem. Soc.* **127**, 12890 (2005).
- ⁵²I. Greenfeld, A. Arinstein, K. Fezzaa, M. H. Rafailovich, and E. Zussman, *Phys. Rev. E* **84**, 041806 (2011).
- ⁵³A. Petrozza, D. Fazzi, I. Avilov, D. Beljonne, R. H. Friend, and J.-S. Kim, *J. Phys. Chem. C* **116**, 11298 (2012).